INERTIAL SUPPORT IMPLEMENTATION IN VARIABLE SPEED PMSG WIND TURBINES

A THESIS SUBMITTED TO
THE GRADUATE SCHOOL OF NATURAL AND APPLIED SCIENCES
OF
MIDDLE EAST TECHNICAL UNIVERSITY

BY

ERENCAN DUYMAZ

IN PARTIAL FULFILLMENT OF THE REQUIREMENTS
FOR
THE DEGREE OF MASTER OF SCIENCE
IN
ELECTRICAL AND ELECTRONICS ENGINEERING

DECEMBER 2018

Approval of the thesis:

INERTIAL SUPPORT IMPLEMENTATION IN VARIABLE SPEED PMSG WIND TURBINES

submitted by **Erencan Duymaz** in partial fulfillment of the requirements for the degree of **Master of Science in Electrical and Electronics Engineering Department, Middle East Technical University** by,

Prof. Dr. Gülbin Dural Ünver
Dean, Graduate School of **Natural and Applied Sciences**

Prof. Dr. Bölüm Başkanı
Head of Department, **Electrical and Electronics Engineering**

Ozan KEYSAN
Supervisor, **Department of Electrical and Electronics Engineering, METU**

Examining Committee Members:

Prof. Dr. Jüri
JüriBölüm, METU

Prof. Dr. Jüri
JüriBölüm, METU

Prof. Dr. Jüri
JüriBölüm, METU

Assoc. Prof. Dr. Jüri
JüriBölüm, METU

Assist. Prof. Dr. Jüri
JüriBölüm, Ankara University

Date:

I hereby declare that all information in this document has been obtained and presented in accordance with academic rules and ethical conduct. I also declare that, as required by these rules and conduct, I have fully cited and referenced all material and results that are not original to this work.

Name, Last Name: Erencan Duymaz

Signature :

ABSTRACT

INERTIAL SUPPORT IMPLEMENTATION IN VARIABLE SPEED PMSG WIND TURBINES

Duymaz, Erencan
M.S., Department of Electrical and Electronics Engineering
Supervisor : Ozan KEYSAN

December 2018, 45 pages

Abstract

Keywords: Keyword1, Keyword2...

ÖZ

BAŞLIK

Duymaz, Erencan
Yüksek Lisans, Elektrik ve Elektronik Mühendisliği Bölümü
Tez Yöneticisi : Ozan KEYSAN

Aralık 2018 , 45 sayfa

Özet Türkçe

Anahtar Kelimeler: AnahtarKelime1, AnahtarKelime2...

İthafen...

ACKNOWLEDGMENTS

Teşekkür edilecekler

TABLE OF CONTENTS

ABSTRACT v

ÖZ vi

ACKNOWLEDGMENTS viii

TABLE OF CONTENTS ix

LIST OF TABLES xii

LIST OF FIGURES xiii

LIST OF ABBREVIATIONS xv

CHAPTERS

1 INTRODUCTION 1

1.1 Global Renewable Energy Status 1

1.1.1 EU 2020 Goals 3

1.1.2 Wind Energy Status 4

1.2 Global Renewable Energy Future 4

1.3 Renewable Energy Problems 6

1.4 Literature Review 7

1.5 Thesis Motivation 9

2 POWER SYSTEM FREQUENCY STABILITY 11

2.1 Synchronous Generator and Synchronous Speed 11

2.2 Swing Equation 12
2.3 Frequency in Power Systems 13
2.3.1 Primary Frequency Control 14
2.3.2 Secondary and Tertiary Control 15
3 WIND TURBINE MODELLING 17
3.1 Variable Speed PMSG Wind Turbines 17
3.1.1 Aerodynamic Model 18
3.1.1.1 Pitch Angle Control 19
3.1.2 Gearbox 20
3.1.3 Permanent Magnet Synchronous Generator 21
3.1.4 Machine Side Converter 22
3.1.5 Grid Side Converter 23
3.2 Synthetic Inertia Implementation 25
3.2.1 Synthetic Inertia Activation Schemes 26
3.2.2 Source of the Inertial Support 27
4 VALIDATION IN TEST CASE 29
4.1 P.M.Anderson 9 Bus Test Case 29
4.1.1 System Properties 29
4.1.2 Load Flow Analysis for Base Case 30
4.1.3 Base Case Frequency Response for Additional Load Connection 31
4.2 Modified Case 34
4.2.1 Load Flow Analysis for Modified Case 34

4.2.2 Modified Case Frequency Response for Additional Load Connection 35

4.3 Decommissioned Case 37

4.3.1 Load Flow Analysis for Decommissioned Case . . 37

4.3.2 Decommissioned Case Frequency Response for Additional Load Connection 38

REFERENCES 41

APPENDICES

A EK A 45

A.1 Örnek Kısım 45

LIST OF TABLES

TABLES

Table 1.1 Comparison of Different Type of Generators for Inertial Response Behaviour 8

Table 4.1 Generator Properties of Test System 29

Table 4.2 Load Properties of Test System 30

Table 4.3 Load Flow Results in Base Case 31

Table 4.4 System Dynamical Properties 31

Table 4.5 Load Flow Results for Modified Case 35

Table 4.6 System Dynamical Properties 38

Table 4.7 Load Flow Results for Decommissioned Case 38

LIST OF FIGURES

FIGURES

Figure 1.1 Installed Renewable Energy Capacity of Leading Countries in 2016 1

Figure 1.2 Renewable Energy Production of Leading Countries in 2016 2

Figure 1.3 Average Renewable Energy Generation per MW in 2016 2

Figure 1.4 Renewable Targets of EU Member States [2] 3

Figure 1.5 Wind Power Capacity of Leading Countries in 2016 4

Figure 1.6 Wind Power Production of Leading Countries in 2016 5

Figure 1.7 Renewable energy share in total energy consumption by EU for 2015, 2020 targets and 2030 potential according to REmap [3] 5

Figure 1.8 Renewable energy shares for 2010, 2030 Reference Case and 2030REmap [4] 6

Figure 2.1 Damper windings in a synchronous generator [5] 11

Figure 2.2 Frequency behaviour in electric grid with the water level in a container analogy [6] 14

Figure 3.1 Variable Speed Geared Wind Turbine Model 17

Figure 3.2 Power Coefficient Variation with Tip Speed Ratio under Zero Pitch Angle 19

Figure 3.3 Power Coefficient Variation for Two Different Pitch Angle 20

Figure 3.4 Pitch Angle Control Diagram 20

Figure 3.5 Gearbox Modelling 21

Figure 3.6 Machine Side Control Diagram 23

Figure 3.7 Grid Side Control Diagram 24

Figure 3.8 Modified MSC for Inertial Support 26

Figure 4.1 P.M.Anderson Test Case 30

Figure 4.2 Location of the Additional Load 32

Figure 4.3 Generator Frequencies for 10% Load Connection 33

Figure 4.4 Frequencies in Generator 1, Load A and Load B 33

Figure 4.5 Modified System Single Line Diagram 34

Figure 4.6 Comparison of Base Case and Modified Case Frequencies 36

Figure 4.7 Comparison of Base Case and Modified Case Frequencies 36

Figure 4.8 Comparison of Base Case and Modified Case Frequencies 37

Figure 4.9 Comparison of Base Case,Modified Case and Decommissioned Case Frequency Responses 39

Figure 4.10 Comparison of Base Case,Modified Case and Decommissioned Case RoCoFs 39

LIST OF ABBREVIATIONS

AC	Alternating Current
AGC	Automatic Generation Control
DC	Direct Current
DFIG	Doubly Fed Induction Generator
FSIG	Fixed Speed Induction Generator
GSC	Grid Side Converter or Controller
IGBT	Insulated Gate Bipolar Transistor
LSC	Line Side Converter or Controller
LVRT	Low Voltage Ride-Through
MOSFET	Metal Oxide Semiconductor Field Effect Transistor
MSC	Machine Side Converter or Controller
PI	Proportional-integral
PLL	Phase Lock Loop
PMSG	Permanent Magnet Synchronous Generator
RoCoF	Rate of Change of Frequency

CHAPTER 1

INTRODUCTION

1.1 Global Renewable Energy Status

Renewable energy is still one of the hottest topics in the power area. The share of the renewable energy systems has been reached significant levels. At the end of 2017, the renewable power capacity has reached 2179 GW throughout the world including hydro power plants [7]. Fig. 1.1 shows the installed renewable energy capacity for leading countries at the end of 2016 and 2017 [1], [7]. China, USA, Brazil and Germany constitutes almost half of the world total capacity. China has the biggest installed renewable capacity so far and increased its capacity by 73 GW in 2017 which is very close to the whole installed electrical power of the Turkey. This indicates the severity of the growing renewable demand.

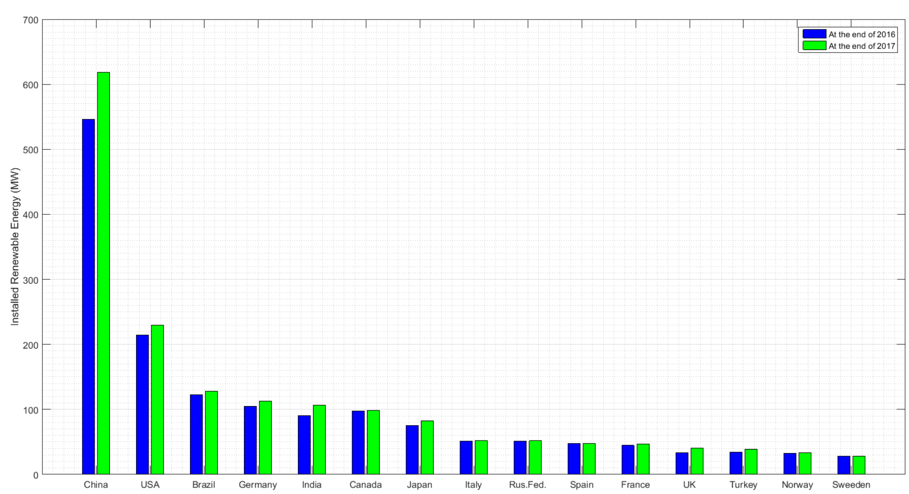

Figure 1.1: Installed Renewable Energy Capacity of Leading Countries in 2016

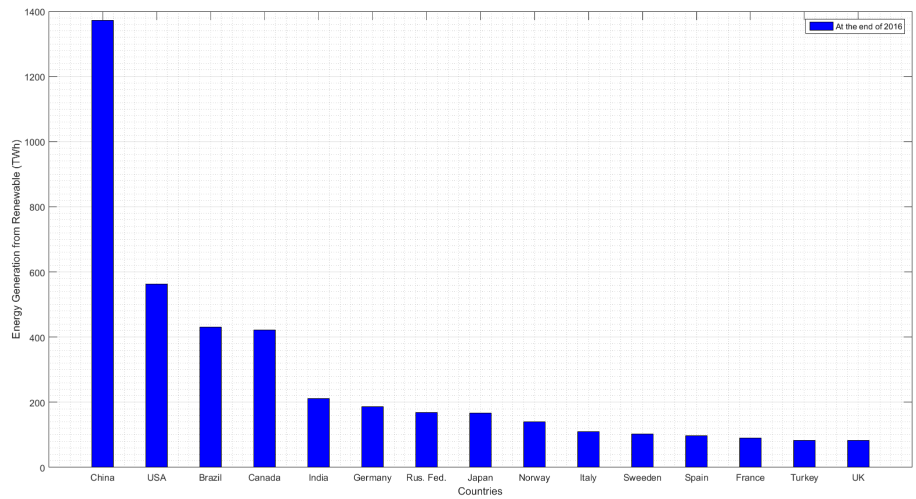

Figure 1.2: Renewable Energy Production of Leading Countries in 2016

Fig. 1.2 shows the energy production from renewable energy systems InternationalRenewableEnergyAgency2017. It is obvious that China, USA and Brazil produces highest amount of energy from renewable since they already have the highest installed capacity. However, India and Canada produces more energy than Germany even though Germany has more installed renewable capacity. This result is due to the fact that renewable energy production is dependent on parameters such as solar radiation and wind speed depending on the renewable source. Fig. 1.3 shows average energy generation from renewable energy sources per MW in 2016 [1]. For a MW renewable energy system, Germany produces the lowest amount of energy meanwhile Canada and Norway produce highest amount among these countries.

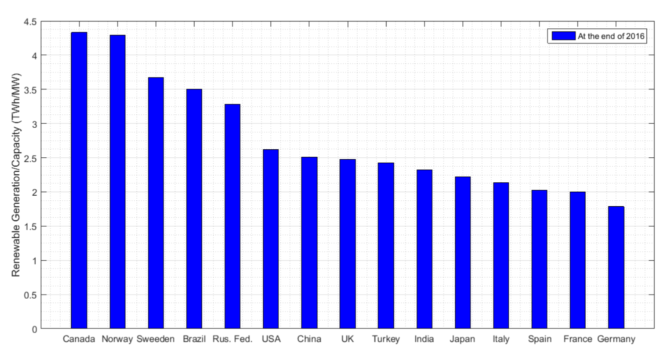

Figure 1.3: Average Renewable Energy Generation per MW in 2016

1.1.1 EU 2020 Goals

In 2008, 20 20 by 2020-Europe's Climate Change Opportunity report has been released by EU Commission and two key targets are set for 2020 [8]:

- At least 20 % reduction in greenhouse gases (GHG) by 2020
- Achieving 20% renewable energy share in energy consumption of EU by 2020

The Renewable Energy Directive is published in 23 April 2009. This directive has set national binding targets for EU countries in order to accomplish the 20% renewable energy target for EU and 10 % target for the renewable energy usage in the transport. [9] As a result, each EU country has been determined their national action plans. In order to achieve the 20 % target, each member state determine their own targets ranging from 10% in Malta to 49% in Sweeden. According to the latest release by Eurostat, renewable share of the EU in energy consumption has reached 17 % in 2016 [2]. Moreover, eleven of EU member states has already achieved their 2020 targets. Renewable shares of EU members are shown in Figure 1.4.

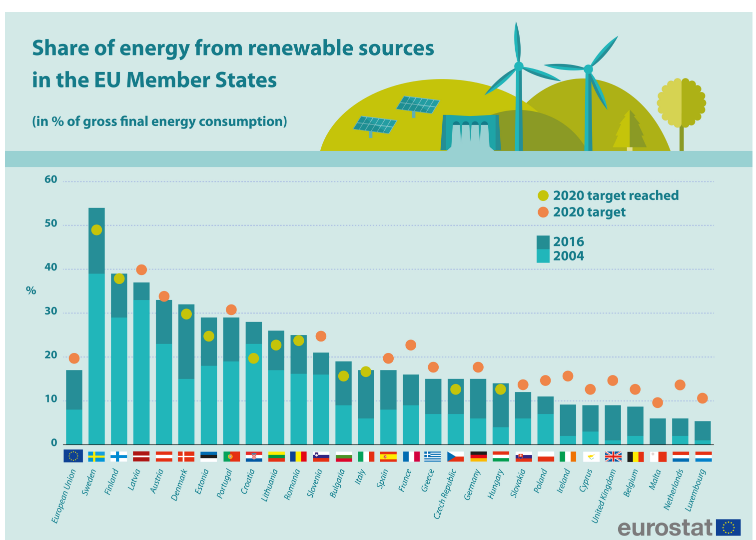

Figure 1.4: Renewable Targets of EU Member States [2]

1.1.2 Wind Energy Status

Wind power has the highest share in the installed renewable energy capacity except for hydro power. The wind power capacity at the end of 2016 has reached 514 GW worldwide [7]. The wind power capacity of the leading countries is shown in the Fig. 1.5. As in the case of total installed renewable energy capacity, China and USA have also the highest installed capacities in the wind power capacity. The energy

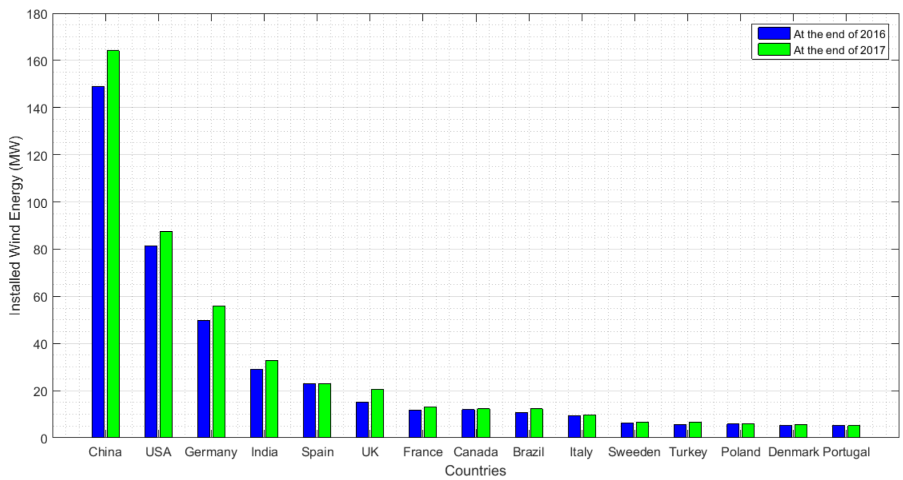

Figure 1.5: Wind Power Capacity of Leading Countries in 2016

production from wind energy is shown in the Figure 1.6. Even though China has the highest wind power capacity, USA generates more energy from wind than any other country.

1.2 Global Renewable Energy Future

The share of renewable energy is increasing each passing day. Today, reports arguing the possibility of even 100% renewable energy region by region is published [10]. The renewable energy reports estimate the share of renewable energy in the total energy consumption for 2030 and 2050. Figure 1.7 shows the EU renewable energy share for 2030. Moreover, the report published by IRENA (International Renewable Energy Agency) estimates the share of renewable energy in EU as 24% by 2030 which is below proposed target of 27% [4]. Renewable shares of REmap countries in 2010,

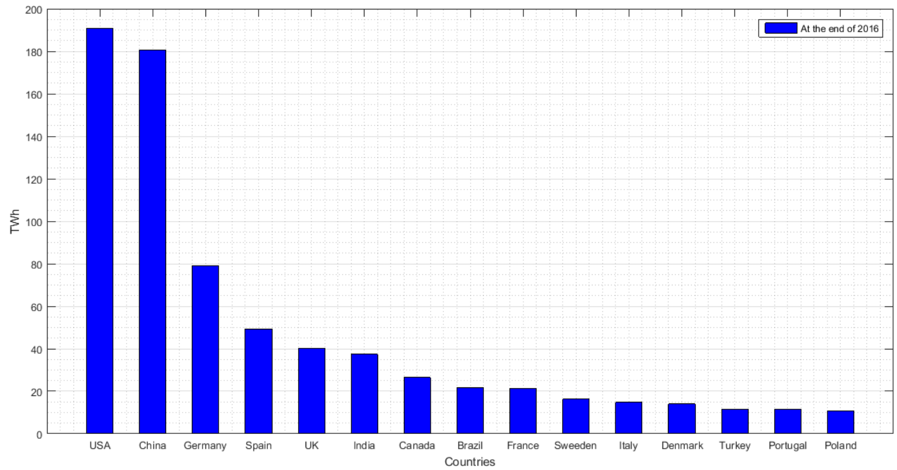

Figure 1.6: Wind Power Production of Leading Countries in 2016

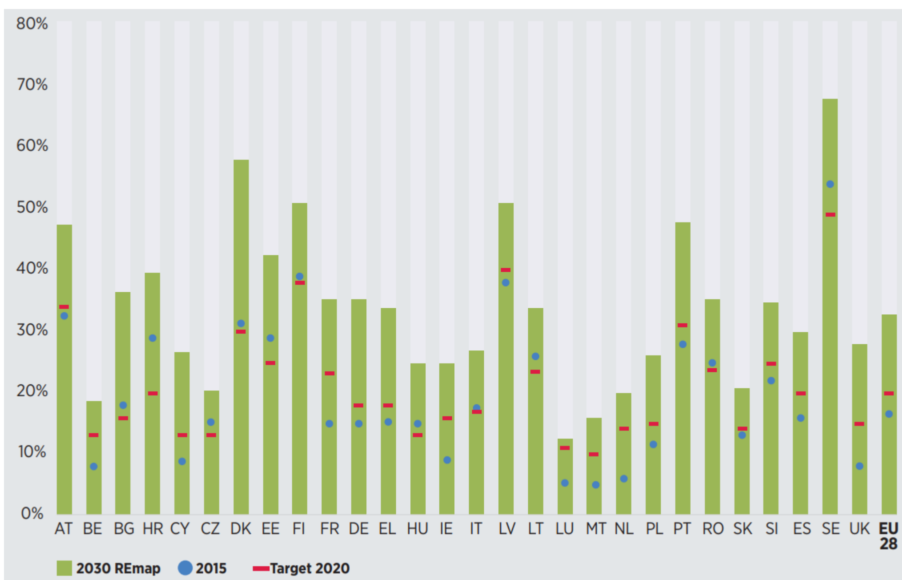

Figure 1.7: Renewable energy share in total energy consumption by EU for 2015, 2020 targets and 2030 potential according to REmap [3]

2030 reference case and 2030REmap and the world average is also shown in Figure 1.8. The only country whose renewable energy decreases in the 2030 is Nigeria. The reason is the main source of energy in Nigeria is biogas for the time being. However, the renewable share is expected to decrease dramatically as the industry switches to natural gas.

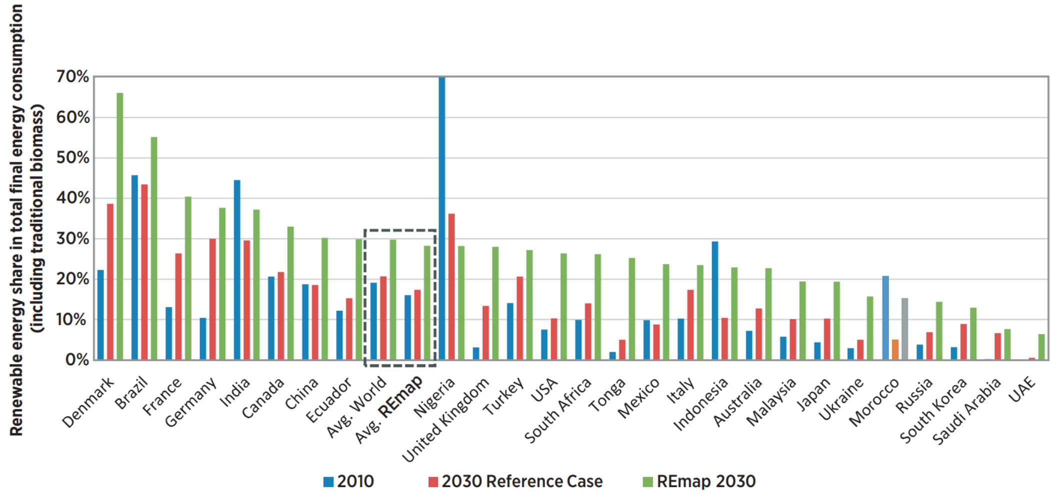

Figure 1.8: Renewable energy shares for 2010, 2030 Reference Case and 2030REmap [4]

1.3 Renewable Energy Problems

It is an undeniable fact that renewable energy systems are advantageous in terms of global warming and carbon dioxide emission. Nonetheless, they also have disadvantages to the system operators due to intermittent energy generation. With the large penetration of intermittent sources, electric grid will face with transmission system issues as overloaded transmission lines, changes on the protection and control in the distribution system, greater level of power-factor control and low voltage ride-through (LVRT) requirements [11].

Another challenge of renewable energy systems is the power system frequency stability. Since the frequency of the power system depends on the balance between generation and consumption, grid operators are responsible for adjusting the generation in order to maintain a constant frequency. However, the renewable energy generation is strictly dependent on the renewable source i.e. solar radiation or wind speed. Therefore, renewable systems makes the system operation harder due to their intermittent and uncertain power generation profiles. Moreover, as the renewable systems with power electronics interface increase in the electricity grid, the grid equivalent inertia decreases. In [12], the reduced grid inertia due to the high DFIG wind turbine penetration is emphasized. Moreover, the results of the reduced grid inertia following a disturbance is listed as:

- increased effective aggregated angular acceleration of synchronous machines which require high restoring forces
- high rate of change of frequency and hence, decreased frequency nadir

It should be noted that this problem is not specific to DFIG wind turbines but renewable energy systems which are connected to grid with power electronics. Conventional synchronous generators rotates with synchronous speed which is proportional to grid frequency. If the grid frequency decreases, then the synchronous speed also decreases. In this case, the generator active power is increased inherently due to kinetic energy extraction from the generator inertia. The increase in active power provides action time for primary controllers and crucial for frequency stability. Type-1 and Type-2 wind turbines are directly connected to grid. Hence, the frequency deviations affects the active power output of such wind turbines [13]. Nonetheless, active power output of renewable energy systems with power electronics such as Type-3 and 4 wind turbines and photovoltaic systems is not affected from the grid frequency deviations. Therefore, these system have no contribution to the grid inertia whether the system includes inertia or not. Hence, the aggravated grid inertia is reduced with the penetration of renewable energy sources. The comparison for different type of generators is given in [14] and listed in Table 1.1. Another reason for the decrease in the grid inertia is the de-commitment or dispatch of the conventional sources due to economic concerns. Since the renewable energy has the lowest cost for energy production, it preferred instead of conventional generators. As a result, conventional generators are dispatched to a lower generation profile or taken-off from operation.

Type of the generator	**Inertial Response Behaviour**
Conventional Synchronous Generator	++
Fixed Speed Induction Generator (FSIG)	+
Doubly Fed Induction Generator (DFIG)	-
Variable Speed Wind Turbine Generator (Connected with Full Scale Power Electronics)	None

Table 1.1: Comparison of Different Type of Generators for Inertial Response Behaviour

1.4 Literature Review

Studies regarding inertial support date back to early 2000s. In the study [15], the effect of the increasing wind energy penetration has been investigated. The study concludes that increasing share of wind energy increases the primary reserve requirement for the successful grid operation. The increased frequency deviations, especially in light load conditions (high wind generation with low consumption scenario) can be mitigated in the system as long as the wind generation provides inertia support. Study in [16] states that DFIG wind turbines are de-coupled from power system resulting in no contribution to system inertia. A supplementary loop is proposed for reinstating the machine inertia. Moreover, in [17], performance of the supplementary control loop is evaluated with the comparison of the inertial support of a fixed-speed wind turbine. The proposed control loop has been validated in [18] and compared with the droop control in [19].

It is an undeniable fact that renewable energy systems are the most economical way of producing electrical energy due to absence of any fuel cost. Therefore, they are to be operated in their rated power. However, they have to curtail their power in order to leave a margin for droop control. Droop control by wind energy is also studied in the literature. In [13], the inertial support of different type of wind turbines is compared. It is concluded that the Type-4 wind turbines are able to perform better performance for inertial support due to the power electronics interface. Moreover, combination of inertial support and droop control produces better results in these wind turbines.

1.5 Thesis Motivation

The frequency of the electric grid depends on the balance between generation and consumption. Grid operators are responsible for maintaining this balance so that frequency of the grid is maintained between allowed dead-band. In order to achieve this purpose, power generation is adjusted according to the consumption value. However, the balance between supply and demand might be disturbed with unintentional generator trip or instant load connections. Grid frequency decreases such instants until the generation is increased to arrest the frequency. Inertia of the electric grid provides additional power from the stored kinetic energy and avoid the system frequency from decreasing down very fast. That is called as inertial support and it is very important for power system frequency stability.

Although renewable energy systems are beneficial for environmental concerns and lower energy cost, higher renewable penetration also brings operational challenges for system operators. One of the most important problem that comes with renewable energy is the power system frequency stability. With the high renewable penetration, grid aggravated inertia decreases. As a result, grid frequency deviates steeper for disturbances. To avoid steeper frequency declines in the grid, all generation technologies should provide inertial support for the frequency disturbances.

Wind energy systems, especially variable speed wind turbines with full scale power electronics are the most promising renewable energy systems that can contribute to grid frequency stability thanks to their high inertia in their blades and generator and also their back-to-back converters that give ability to control its active power. Therefore, wind energy conversion systems are required to participate in ancillary services for frequency stability in order to reach a stable power system network in the upcoming future.

CHAPTER 2

POWER SYSTEM FREQUENCY STABILITY

2.1 Synchronous Generator and Synchronous Speed

Synchronous machines produce torque only in synchronous speed. This is why they are equipped with damper windings which are basically induction machine windings. If the frequency of grid changes, damper windings create a torque which creates a force to synchronize the speed to the grid frequency. Two type of damper windings are given in Fig. 2.1.

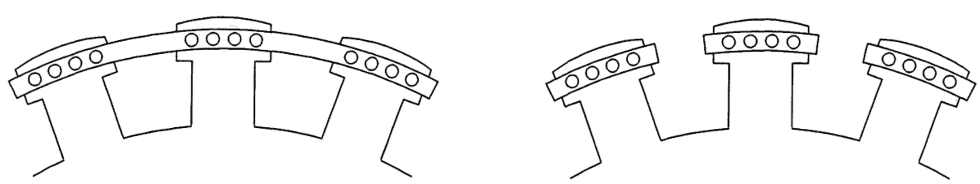

(a) continuous damper

(b) non-continuous damper

Figure 2.1: Damper windings in a synchronous generator [5]

The synchronous machines keep their operation in the synchronous speed thanks to the damper windings in the rotor. Relation between grid frequency and the synchronous speed is given in Eq. (2.1) in terms of rpm. [5]. This equation can be better observed in Eq (2.3).

$$n_s = \frac{120f}{p_f} \tag{2.1}$$

$$n_s = \frac{60}{2\pi}\omega_{syn} \tag{2.2}$$

$$\omega_{syn} = \frac{4\pi f}{p_f} \tag{2.3}$$

where n_s is the synchronous speed in rpm, f is the grid frequency in Hz, p_f is the number of poles of the generator and ω_{syn} is the synchronous angular speed in rad/s.

2.2 Swing Equation

Speed in synchronous machines changes according to the net torque acting on the rotor. Therefore, the speed is maintained constant unless there is no difference between mechanical and electromechanical torque. The equation of motion is given in Eq. (2.4) where J is aggravated moment of inertia of the generator and the turbine in kgm^2,T_m and T_e are mechanical and electromechanical torques in Nm.

$$J\frac{d\omega_m}{dt} = T_m - T_e = T_a \tag{2.4}$$

In power system network, the power ratings of the generators and corresponding moment of inertia values varies. Hence, it is more convenient to use inertia constant, H whose unit is seconds and varies between 2 and 9 [5]. Inertia constant is defined as the ratio of kinetic energy stored in the inertia to the power rating of the generator as in Eq. (2.5) where ω_{0m} denotes the rated angular velocity of generator in rad/s and S_{base} is the rated apparent power in VA.

$$H = \frac{\frac{1}{2}J\omega_{0m}^2}{S_{base}} \tag{2.5}$$

Substituting Eq. (2.5) into Eq. (2.4) and replacing units to per-unit quantities yield the relation of frequency with power and inertia constant as in Eq. (2.10).

$$J = \frac{2H}{\omega_{0m}^2}S_{base} \tag{2.6}$$

$$\frac{2H}{\omega_{0m}^2}S_{base}\frac{d\omega_m}{dt} = T_m - T_e \tag{2.7}$$

$$\frac{2H}{\omega_{0m}^2} S_{base} \omega_m \frac{d\omega_m}{dt} = P_m - P_e \tag{2.8}$$

$$2H \frac{\omega_m}{\omega_{0m}} \frac{d(\omega_m/\omega_{0m})}{dt} = \frac{P_m - P_e}{S_{base}} \tag{2.9}$$

$$2H \overline{\omega_m} \frac{d\overline{\omega_m}}{dt} = \overline{P_m} - \overline{P_e} \tag{2.10}$$

2.3 Frequency in Power Systems

The frequency in a power system is related to the speed of the synchronous generators and changes according to the swing equation. The frequency of the each generator is not the same in the network since each generator does not have the same speed. There are always fluctuations in the power system. However, the network can be assumed as a single generating unit by neglecting this assumption. The swing equation basically investigates the relation between mechanical and electromechanical powers and the rate of change of angular speed of a generator. Therefore, the speed of an generator remains constant if the mechanical and electromechanical powers are equal.
If the electricity grid is considered as a single generator, the inertia of the equivalent generator is aggravated from each generator in the network. In this case, average frequency in the network can be found as in Eq. (2.11)

$$2H_{sys} \overline{f_{sys}} \frac{d\overline{f_{sys}}}{dt} = \overline{P_m} - \overline{P_e} \tag{2.11}$$

where P_m is the aggravated mechanical input power of the generators meanwhile P_e is the aggravated electromechanical output power. In other words, the system frequency depends on the balance between generation and consumption. Note that generation means the input mechanical power of the generators.

The behaviour of the frequency in electric grid is depicted in Fig. 2.2. As it can be seen from the water level in a container analogy, the frequency of the system is dependent on the in-flow and the out-flow. Therefore, in the electricity grid, frequency increases as the aggravated input power is higher than the aggravated output power. Note that, the direction of the frequency is dictated by this balance. Having a constant

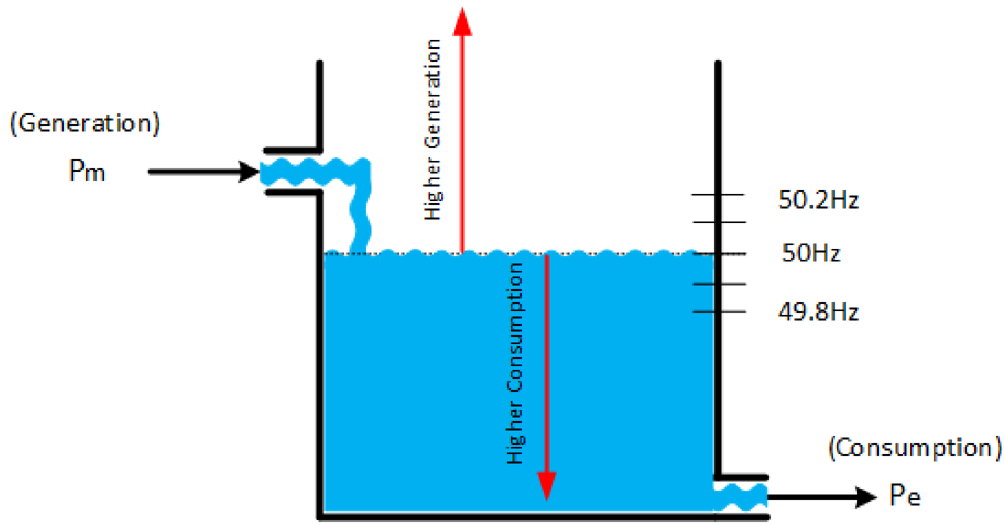

Figure 2.2: Frequency behaviour in electric grid with the water level in a container analogy [6]

49.8Hz frequency does not mean that consumption is higher than generation. If the frequency is constant, then the input mechanical power is equal to output power.

2.3.1 Primary Frequency Control

Having a constant frequency is one of the most important responsibilities of a system operator. In order to have a constant frequency, supply is being adjusted according to the demand continuously. By doing so, the system frequency varies between a band-gap. The variation depends on the disturbances which are generally a sudden generation outage or instant load connection. The size of the disturbance determines the severity of the frequency change and there are three main mechanisms to arrest the frequency changes in the system.
Following generator outage or sudden load connection event, frequency start decreasing. The slope of the frequency is dependent on the severity of the event by means of power and the available inertia of the power system. Such frequency disturbance requires increased input power. However, the increase in the input mechanical power should be activated very fast and should be automated. This responsibility is assigned to generating units with primary control. The active power generation of these units is increased or decreased by the governor depending on the network frequency di-

rection. Note that each generator in the power system does not necessarily perform primary control function. In this case, their active power generation is independent from the network frequency. Hence, the decrease in the frequency is arrested by the primary frequency control. The primary controllers act during a few seconds following a disturbance. They keep their operation up to 30 minutes.

2.3.2 Secondary and Tertiary Control

The frequency is recovered back to nominal value with the Secondary Frequency Control action. This controller might be a single or multiple centres that monitor the frequency and adjust the generation accordingly. They are also called as Automatic Generation Control (AGC) systems and their action takes a few minutes. The final frequency control mechanism is the Tertiary Frequency Control. If the frequency is not recovered back to nominal value with the secondary controllers, tertiary frequency controllers manually activates the load shedding which is an undesired situation by the network operator. However, it is an emergency case which might result in blackout and requires immediate action.

CHAPTER 3

WIND TURBINE MODELLING

3.1 Variable Speed PMSG Wind Turbines

The share of variable speed PMSG wind turbines is increasing worldwide due to the high efficiency and torque density. This type of wind turbines are equipped with full-scale power electronics which enable the turbine to have wide speed range. Even though the price of the permanent magnet fluctuates with time, the reliability and high efficiency of this type of turbine increase its share in the market.

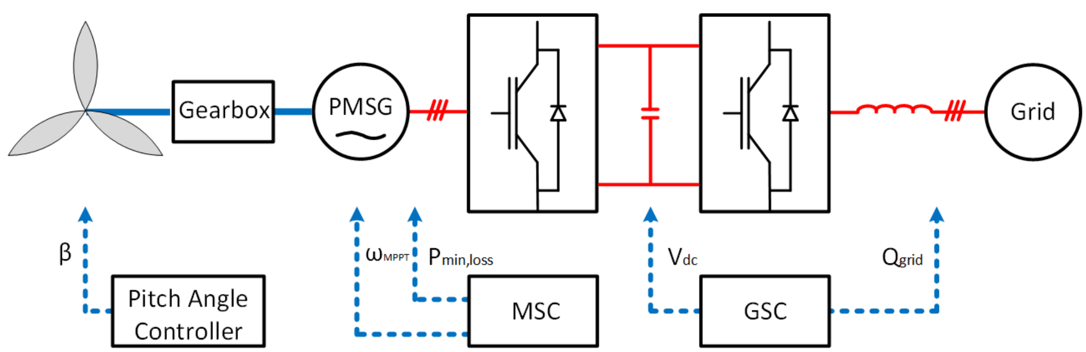

Figure 3.1: Variable Speed Geared Wind Turbine Model

Fig. 3.1 shows the modelling of variable speed PMSG wind turbine. The source of the power in these systems is the wind itself. The power is captured from the wind with the help of three-blade turbine. Three-blade turbine is the aerodynamic part of the system and it applies a aerodynamic torque to gearbox. In fact, this torque is the source of the movement and dictates the direction of the movement. Aerodynamic torque is applied to gearbox which establishes the connection between turbine and generator. In variable speed wind turbines, stator of the PMSG is not directly connected to grid. A back-to-back converter is used between generator and the electrical grid to ensure that the turbine speed is independent from the grid frequency. The converter which is connected to PMSG is called Machine Side Converter (MSC) meanwhile the one connected to grid is called Grid Side Converter(GSC). Moreover, GSC is connected to grid with a filter in order to filter out high frequency currents due to switching action.

3.1.1 Aerodynamic Model

Aerodynamic model is the sub-model that captures power from the wind. The output of this block is the aerodynamic torque that rotates the turbine. However, the wind speed is not the only input. Turbine speed and pitch angle are also the inputs of the system since they affect the mechanical power that is captured from the wind.

The aerodynamic power of wind is given in Eq. (3.1) where ρ_{air} is air density in kg/cm^3, R is the blade radius in m abd v_{WIND} is the wind speed in m/s. Note that this is the available power of the air that is striking the turbine swept area and it is not possible to extract that amount of energy. Otherwise, the air would be standstill behind the wind turbine [20].

$$P_{WIND} = 0.5\rho_{air}\pi R^2 v_{WIND}^3 \tag{3.1}$$

The wind turbine captures a fraction of the available wind power that is denominated as power coefficient C_p. Therefore, turbine power captured from wind can be found with the Eq. (3.2).

$$P_{TUR} = C_P P_{WIND} \tag{3.2}$$

Power coefficient determines the amount of power and it is a non-linear function of the tip speed ratio, λ and pitch angle, β. Tip speed ratio is a parameter proportional with turbine speed. It can be defined as the ratio of the speed in the turbine tip to the wind speed as in the Eq. (3.3). Power coefficient for a specific tip speed ratio and pitch angle can be found with the Eq. (3.4) and (3.5) where c_1 is 0.5176, c_2 is 116, c_3 is 0.4, c_4 is 5, c_5 is 21 and c_6 is 0.0068 [21].

$$\lambda = \frac{\omega_{tur} R}{v_{WIND}} \tag{3.3}$$

$$C_p(\lambda, \beta) = c_1(c_2/\lambda_i - c_3\beta - c_4)e^{-c_5/\lambda i} + c_6\lambda \tag{3.4}$$

$$\frac{1}{\lambda_i} = \frac{1}{\lambda + 0.08\beta} - \frac{0.035}{\beta^3 + 1} \tag{3.5}$$

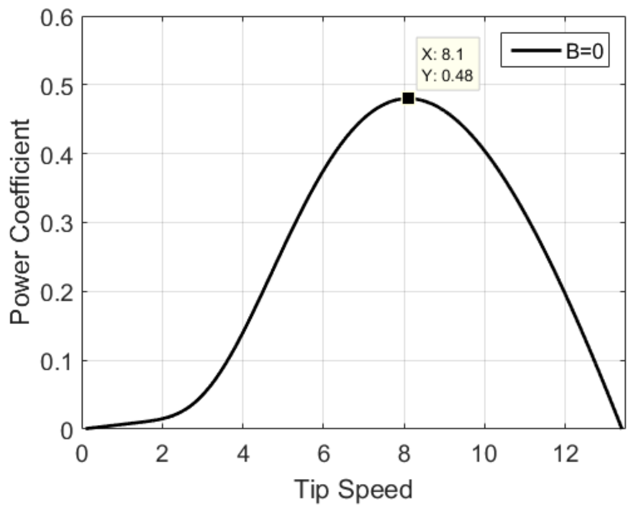

Figure 3.2: Power Coefficient Variation with Tip Speed Ratio under Zero Pitch Angle

Variation of power coefficient C_p is given in Fig. 3.2. For the zero pitch angle, power coefficient has the maximum value of 0.48 for the tip speed ratio of 8.1. In order to ensure that the maximum of wind power is extracted, wind turbine should rotate a speed that gives the optimum tip speed ratio.

3.1.1.1 Pitch Angle Control

According to Eq. (3.1), wind power increases with the cube of the wind speed. Hence, wind power increases dramatically for the high wind speeds. In order to decrease power, pitch angle i.e. blade angle is increased. Since the power coefficient, C_p is a function of the pitch angle, β, wind power can be curtailed with increased blade angle. Variation of power coefficient for two different pitch angle is shown in Fig. 3.3. Increasing pitch angle by $1.176°$ decreases power coefficient by 10%.

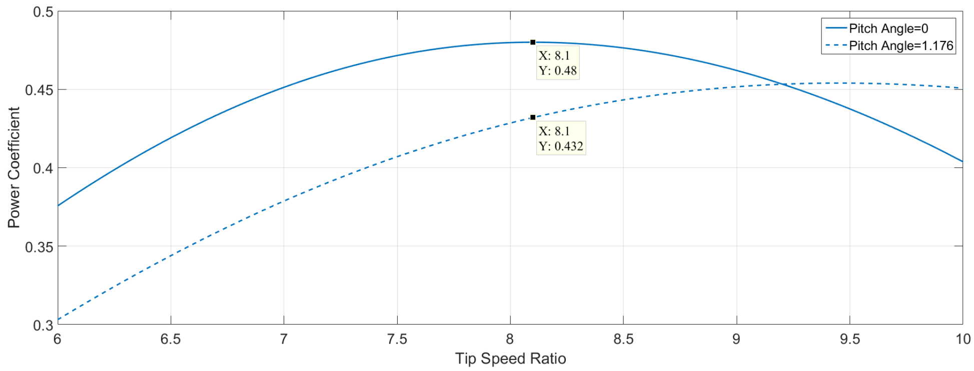

Figure 3.3: Power Coefficient Variation for Two Different Pitch Angle

As long as wind power is below the rated power, the wind turbine is operated in MPPT speed. This is ensured by obtaining optimal tip speed ratio. This means that for zero pitch angle, MPPT speed is increased linearly with wind speed. Before reaching rated power, MPPT speed might reach maximum generator speed. In this case, wind turbine reference speed will be the maximum generator speed. However, turbine speed cannot be decreased down to reference speed when the torque limit is reached. Hence, the pitch angle should be increased to regulate the turbine speed. Pitch angle controller is depicted in Fig. 3.4. Note that the pitch angle is increased when the speed exceeds maximum generator speed. Otherwise, the pitch angle kept as zero.

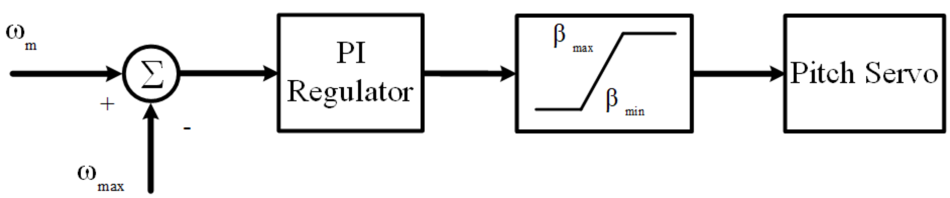

Figure 3.4: Pitch Angle Control Diagram

3.1.2 Gearbox

Variable speed PMSG wind turbines have a gearbox between turbine and generator except for direct-drive wind turbines. The gearbox increases angular speed and decreases the torque in the generator side.By decreasing the rated torque, generator size and cost can be reduced since the generator size is almost proportional to rated torque due to constant shear stress [22]. Moreover, turbine speed is increased to the allowable speed range of the generator which is generally much higher than that of wind turbines. Otherwise, generator should have high pole numbers.

A gearbox model is depicted in Fig. 3.5. They are mainly used for speed and torque conversion. It should be noted that the gearboxes are not full efficient systems. Therefore, the output torque of the gearbox would be lower than the ratio of input torque to gearbox conversion ratio. Direct-drive systems are based on the elimination of the gearbox systems by direct connection between turbine and generator in order to increase efficiency and reliability [23]. In this study, gearbox system is modelled with 100% efficiency.

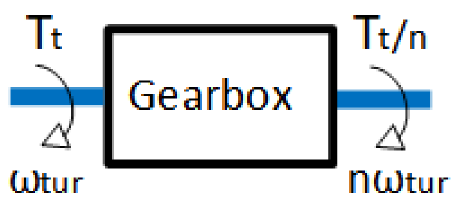

Figure 3.5: Gearbox Modelling

3.1.3 Permanent Magnet Synchronous Generator

PMSGs are generally preferred over electrically excited synchronous generators due to high efficiency due to the fact that absence of electrical excitation on the rotor decreases losses. Besides, slip ring is not needed in the generator which also decrease the maintenance. Dynamical equations of the salient pole PMSG are projected on a reference frame which rotates synchronously with magnet flux and given in Eq. (3.6) and (3.7) where R_1 is stator resistance in Ω, L_{sd} and L_{sq} are d and q axis inductances in H, i_{ad} and i_{aq} are d and q axis currents in A, ω is the electrical angular frequency in rad/s ψ_f is magnet flux linkage in Vs [20].

$$v_{1d} = R_1 i_{ad} + L_{sd}\frac{di_{ad}}{dt} - L_{sq}\omega i_{sq} \tag{3.6}$$

$$v_{1q} = R_1 i_{aq} + L_{sq}\frac{di_{aq}}{dt} + L_{sd}\omega i_{sd} + \omega\psi_f \tag{3.7}$$

Another important PMSG parameter is the power in dq frame. The power expression is given in Eq. (3.8). The electromechanical torque can be found by the relation between power and angular speed. The torque expression is also given in Eq. (3.9) where p is the number of pole pair.

$$P_{elm} = \frac{3}{2}\omega i_{aq}(\psi_f + i_{ad}(L_{sq} - L_{sd})) \tag{3.8}$$

$$T_e = \frac{P_{elm}}{w_m} = \frac{P_{elm}}{w/p} = \frac{3}{2}p i_{aq}(\psi_f + i_{ad}(L_{sq} - L_{sd})) \tag{3.9}$$

Given equations are defined for salient pole machines. If the clyndrical rotor machine is used, the torque equation reduces to the Equation 3.10.

$$T_e = \frac{3}{2}p i_{aq}\psi_f \tag{3.10}$$

3.1.4 Machine Side Converter

Variable speed wind turbines are equipped with the Back-to-Back converters in order to decouple grid frequency and the turbine speed. This gives wind turbine degree of freedom for the rotational speed. In this way, turbine is able to capture the maximum available power from wind. Machine Side Converter (MSC) i.e. Generator Side Converter is the converter that is connected between generator and DC-bus. The three phase generator output AC voltage is converted to DC voltage. Conversion from AC to DC can be achieved by three-arm full bridge converters. This converter can be equipped with uncontrolled, semi-controlled and fully-controlled switches. Fully-controlled switches such as MOSFET,IGBT are commonly used in the industry and gives two control parameters to the user.

Voltages and currents are generally transformed into synchronously rotating reference frame or also called dq frame. Since the frame is rotating in synchronous speed, three-phase phasors are transformed to DC quantities. Therefore, its control becomes easier [24]. Proportional-integral (PI) controllers are associated with the dq control structure due to their satisfactory behaviour interaction to DC variables [25]. Hence, the control in the back-to-back converter is achieved with PI controllers in the dq frame.

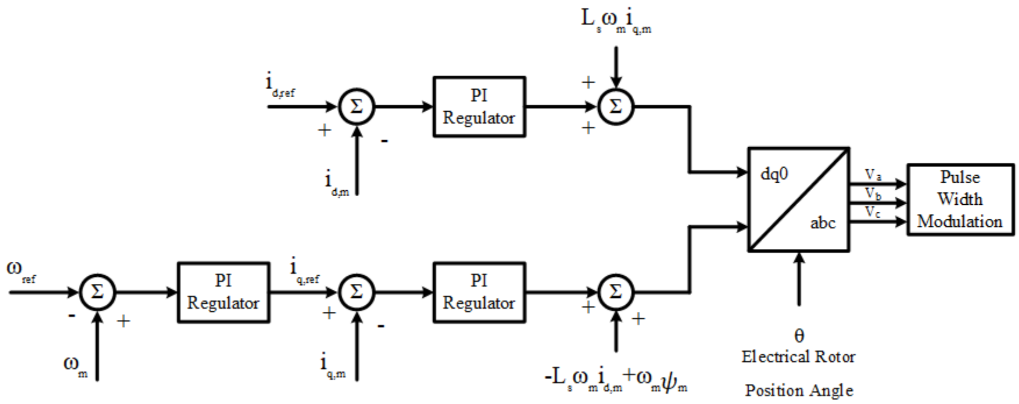

Figure 3.6: Machine Side Control Diagram

The control diagram of the MSC is depicted in Fig. 3.6 according to the study in [26]. In dq frame, it is possible to control two parameters. One of these parameters is the d-axis current. It can be set zero in order to decrease the stator copper losses. The other parameter is the q-axis current that is proportional to the electromagnetic torque as it can be observed in the Eq. (3.10). However, q-axis current or torque is controlled in order to regulate the turbine speed. Therefore, turbine speed is adjusted such that the turbine will capture maximum available power in the wind.

3.1.5 Grid Side Converter

Grid Side Converter (GSC) or Line Side Converter (LSC) is the converter that is connected between DC-link capacitance and grid. GSC works as an inverter that injects current synchronous with grid voltage. Currents and voltages are transformed into synchronously rotating frame that is aligned with the grid voltage. Therefore, d-axis current determines the amount of current which is in phase with the grid voltage meanwhile q-axis current determines amount of current that is out of phase with the grid voltage. In other words, injecting d-axis current injects active power to grid meantime q-axis current injects reactive power to grid.

The responsibility of the GSC is regulating DC voltage and the reactive power injected to grid. The control diagram of the GSC is given in Fig. 3.7. As seen from the figure, DC-bus voltage is regulated by controlling the d axis current. If the DC-bus voltage increases above the reference value, d-axis current reference is increased. As a result, active power increases. Increased active power also decreases the DC-bus voltage level. Reference value of the q-axis current is set to zero in normal operation, consequently unity power factor. For Low Voltage Ride-Through studies, q-axis current is determined according to the reactive power value requirement. [27]

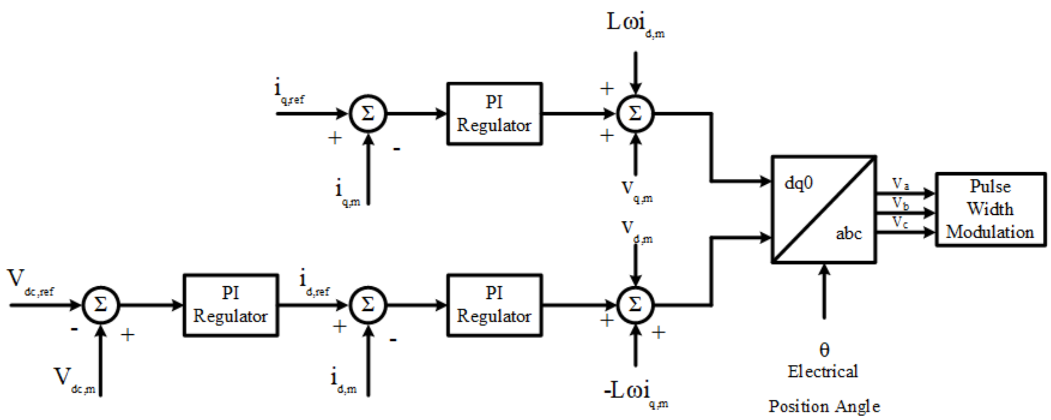

Figure 3.7: Grid Side Control Diagram

GSC is connected to grid through an filter. Therefore, the output voltage of the converter is not equal to the that of grid. The relation between converter voltage, grid voltage and current is derived through Eq. (3.11) to (3.17) where v_c is the converter voltage, v_g is the grid voltage and i_g is the grid current measured in the grid side. As it is observed in Eq (3.16) and (3.17), converter side voltage includes same axis grid voltage and a term proportional to cross axis current which is called cross-coupled term. Therefore, the outputs of the inner PI regulators are compensated and forwarded to Pulse Width Modulation after transformation to three-phase voltages.

$$\overline{v_c} = v_{dc} + jv_{qc} \tag{3.11}$$

$$\overline{v_g} = v_{dg} + jv_{qg} \tag{3.12}$$

$$\overline{i_g} = i_{dg} + ji_{qg} \tag{3.13}$$

$$\overline{v_c} = \overline{v_g} + \overline{i_g}j\omega L \tag{3.14}$$

$$v_{dc} + jv_{qc} = v_{dg} + jv_{qg} + j\omega L(i_{dg} + ji_{qg}) \quad (3.15)$$

$$v_{dc} = v_{dg} - \omega L i_{qg} \quad (3.16)$$

$$v_{qc} = v_{qg} + \omega L i_{dg} \quad (3.17)$$

3.2 Synthetic Inertia Implementation

As explained in Chapter 2 Section 2.2, synchronous generators changes its speed according to the balance between input mechanical and electromechanical powers. The inverse case is also true. In other words, if the frequency changes, the electromechanical power of the generators also change. Synthetic inertia is the method that implements this behaviour on the renew able energy systems. It is possible to change the active power output of the wind turbines if these are connected to grid with full scale power electronics. The increase in the active power should be proportional to change of frequency and the inertia of the renewable energy system. Even though renewable energy system does not have inertia, inertial support with desired inertia constant can be implemented in the system as long as a stored energy exists in the system.

In order to implement synthetic inertia in the system, a relation between frequency and active power of the wind turbine should be constructed. Wind turbine in this study is variable speed wind turbine with full scale power electronics. The speed of the turbine is controlled by MSC such that active power is adjusted.Inertial support modification is depicted in Fig. 3.8. The new value of the active power is determined according to the swing equation. However, the wind turbine in this study is operated with a reference speed rather than a reference power. Therefore, the assigned power value should be used in order to yield the q-axis current reference value. Reference q-axis current is derived between the Eq. (3.18) to Eq. (3.21).

$$P_{new} = (1 + \Delta P) P_{pre} \quad (3.18)$$

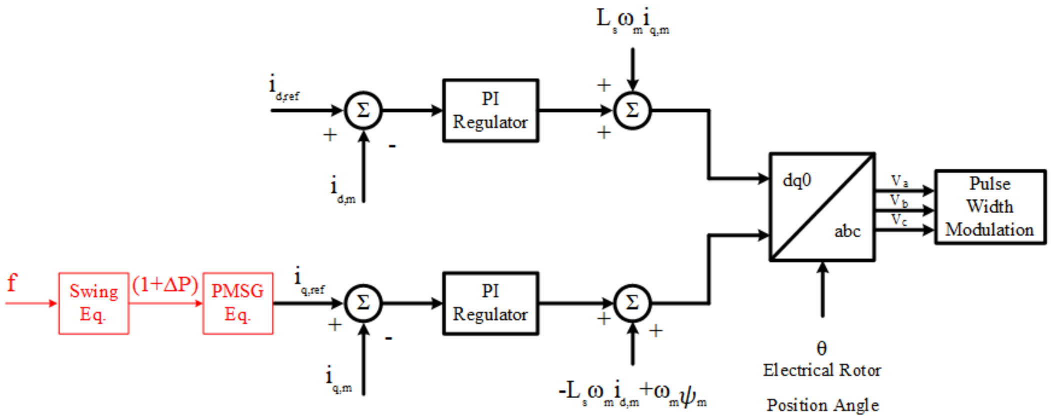

Figure 3.8: Modified MSC for Inertial Support

$$T_{new}\omega_m = (1+\Delta P)T_{pre}\omega_{pre} \tag{3.19}$$

$$\frac{3}{2}p\psi_f i_{q,new}\omega_m = (1+\Delta P)\frac{3}{2}p\psi_f i_{q,pre}\omega_{pre} \tag{3.20}$$

$$i_{q,ref} = i_{q,new} = (1+\Delta P)\frac{i_{q,pre}\omega_{pre}}{\omega_m} \tag{3.21}$$

3.2.1 Synthetic Inertia Activation Schemes

Another issue about inertial support is the time instant to trigger synthetic inertia. In the literature, continuous operation, under-frequency trigger and maximum-frequency gradient are discussed [28]. It is obvious that continuous operation would create oscillations in active power output due to the continuous deviations in grid frequency. This is an unrealistic operation and is used for comparison purposes.

Second activation method is the under-frequency trigger which is the activation when the frequency decreases below a threshold value. It can be used for capturing the time instant for the inertial support. However, power grid might be in a stable point even if the frequency is 49.8Hz. Therefore, this method would be unsuccessful depending on the disturbance event.

Third activation scheme is the maximum-frequency gradient trigger. It uses a controller that is very similar to RoCoF relays and tracks the frequency gradient. Once the frequency gradient is below a threshold value, the synthetic inertia is activated. Since the severity of frequency disturbance event is related to the RoCoF, this activation scheme is the most remarkable scheme [28]. In this study, maximum-frequency gradient is used with a threshold value of 0.1Hz/s.

3.2.2 Source of the Inertial Support

Renewable energy systems convert the energy captured from wind or sun to the electrical energy. Hence, the renewable energy systems cannot determine the amount of power in contrast the conventional systems. A thermal power plant, for instance, adjusts its power output as desired. However, the source of power in renewable energy is constant for a definite wind speed or solar radiation. This is why a spare energy is required in order to change the power output.

Energy stored in DC bus capacitance is the only stored energy in PV systems. The amount of energy is given in Eq. (3.22) and negligible for inertial support studies. In the wind energy systems, there exists huge amount of kinetic energy in wind turbine generator and blades in addition to electrostatic energy. The kinetic energy expression is given in Eq. (3.23). Note that J_{total} is the equivalent inertia in the generator side and ω_m is the speed of the generator.

$$E_{electrostatic} = \frac{1}{2} C_{DC} V_{DC}^2 \tag{3.22}$$

$$E_{kinetic} = \frac{1}{2} J_{total} \omega_m^2 \tag{3.23}$$

Note that the amount of kinetic energy is dependent on the generator speed. Therefore, the stored energy in wind turbines changes according to the generator speed. Moreover, it can also be concluded that the energy is dependent on the wind speed. However, the generator speed is kept constant if the wind speed increases above the rated wind speed.

To illustrate the situation better, the electrostatic energy stored in DC bus and kinetic energy in turbine equivalent inertia are compared for GE2.75-103 wind turbine. The wind turbine has a DC bus capacitance of $27mF$ and $1200V$ DC link voltage. The corresponding electrostatic energy is calculated in Eq. (3.24). The generator speed of the corresponding generator is between $550rpm$ and $1735rpm$. The total turbine inertia is $1058.2kgm^2$ in generator side. The minimum and maximum kinetic energy values are calculated in Eq. (3.25) and (3.26). These values are found out to be 90 and 900 times of the electrostatic energy stored in DC bus capacitance.

$$E_{electrostatic} = \frac{1}{2}27(10^{-3})1200^2 = 19.44kJ \tag{3.24}$$

$$E_{kinetic} = \frac{1}{2}(1058.2)57.6^2 = 1755.17kJ \tag{3.25}$$

$$E_{kinetic} = \frac{1}{2}(1058.2)181.7^2 = 17466kJ \tag{3.26}$$

CHAPTER 4

VALIDATION IN TEST CASE

4.1 P.M.Anderson 9 Bus Test Case

4.1.1 System Properties

In order to understand frequency dynamics better, P.M. Anderson test case has been used in the study. The single line diagram of the system is given in Fig. 4.1. The test case consists of three generators and three loads. Generators in the system are connected to 230 kV high voltage network with transformers.

The biggest generator in the system is a hydro power plant with a power rating of 247.5 MVA. The remaining ones are steam generators. The power ratings of the generators are given in Table 4.1.

Generators	Power Rating (MVA)	Plant Type
Gen 1	247.5	Hydro
Gen 2	192	Steam
Gen 3	128	Steam

Table 4.1: Generator Properties of Test System

The loads in the system are connected directly to the high voltage network. The active and reactive power ratings of the loads are listed in Table 4.2.

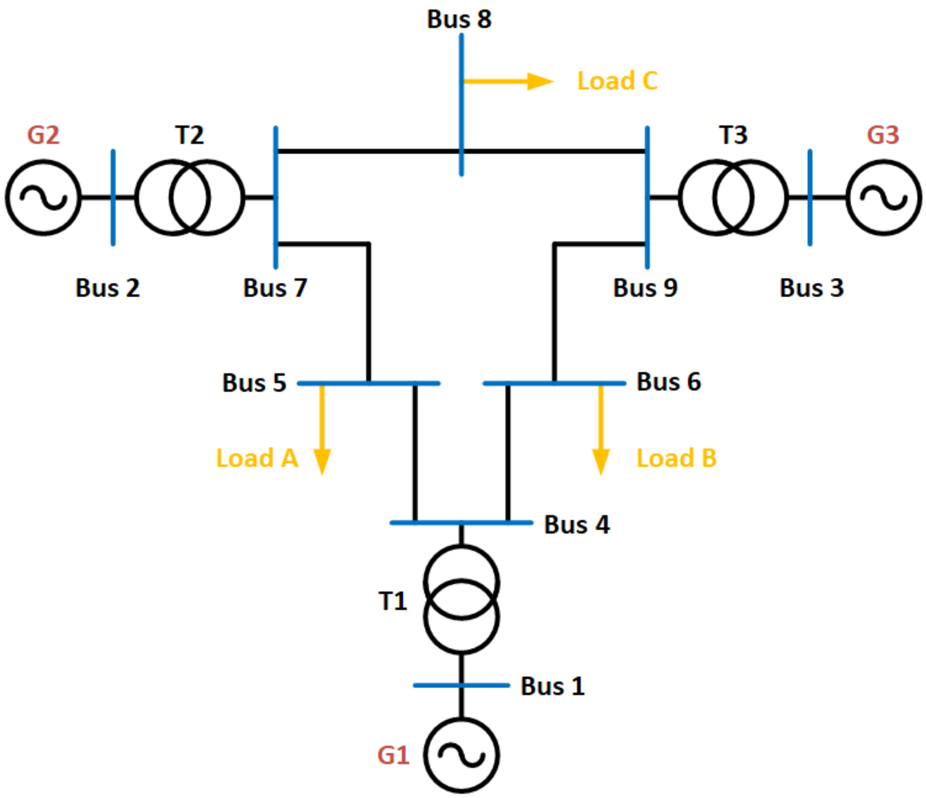

Figure 4.1: P.M.Anderson Test Case

Generators	Active Power (MW)	Reactive Power (MVAr)
Load A	125	50
Load B	90	30
Load C	100	35

Table 4.2: Load Properties of Test System

4.1.2 Load Flow Analysis for Base Case

Successful grid operation requires a load flow analysis in order to ensure that bus voltages are inside the allowed band and power flows are below the power carrying capabilities of the lines. Load flow results are given in Table 4.3.

Bus #	Bus Type	Voltage	Angle	Pg	Qg	Pl	Ql
1	SL	1.04	0	71.65	27.05	0	0
2	PV	1.025	9.28	163	6.65	0	0
3	PV	1.025	4.66	85	-10.86	0	0
4	PQ	1.0258	-2.22	0	0	0	0
5	PQ	0.9956	-3.99	0	0	125	50
6	PQ	1.0126	-3.69	0	0	90	30
7	PQ	1.0258	3.72	0	0	0	0
8	PQ	1.0159	0.73	0	0	100	35
9	PQ	1.0323	1.97	0	0	0	0

Table 4.3: Load Flow Results in Base Case

Total System Load	315 MW
Generator Droop Settings	5%
Stored Kinetic Energy at Nominal Speed	3.305 GWs
Gen 1 Inertia Constant	9.5515 s
Gen 2 Inertia Constant	3.9216 s
Gen 3 Inertia Constant	2.7665 s

Table 4.4: System Dynamical Properties

4.1.3 Base Case Frequency Response for Additional Load Connection

It is obvious that power system networks experience high RoCoF when either high amount of generation trips or high amount of load connects to system. These two main event can be used in the simulation to create frequency disturbances. Since the simulation in Simulink environment slows down with the increasing amount of generators, the disturbances are created with load connections.

System dynamical properties are listed in Table 4.4. Power generation references are determined based on the load flow of powergui toolbox. Machine initialization toolbox is also used to initiate the state of generators in the system. However, the system does not start with the steady state. Still, system goes to steady state within a few seconds. Frequency of the network is disturbed with a load connection in the t=10 seconds in order to observe the frequency stability of the system. For 10% load connection, a load of 31.5 MW is connected to system from Bus 6. Location of the additional load is depicted in Fig. 4.2.

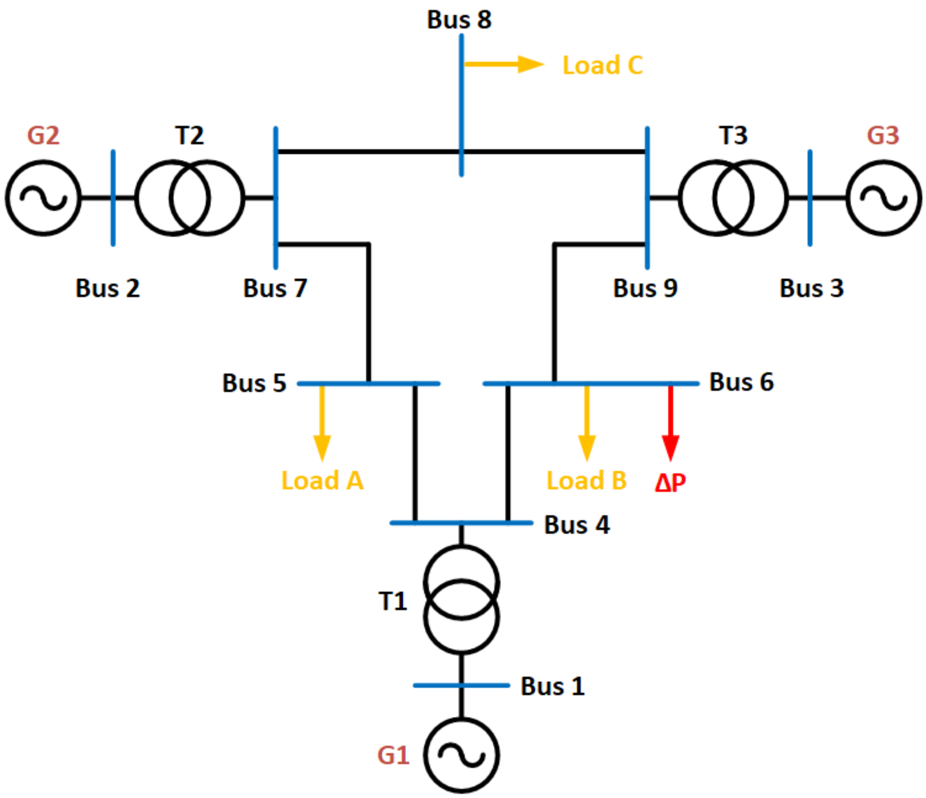

Figure 4.2: Location of the Additional Load

According to the 10% load connection to system, generator frequencies are shown in Fig. 4.3. Frequency of generator 1 is the most smooth one due to its huge inertia constant. Meanwhile, the generator 2 and generator 3 follow the frequency of generator 1 even though they oscillate with each other.

In the system, frequency of Bus 1 can be assumed as constant throughout the network since the system is small enough to assume a single frequency. This assumption can be verified by comparing the frequencies in Buses 1, 5 and 6. Fig. 4.4 shows the frequency of the generator 1 frequency as well as the load frequencies captured with Simulink PLL block. The only difference is the instant following the load connection. The sharp frequency decline delays the PLL loop to capture the frequnecy.

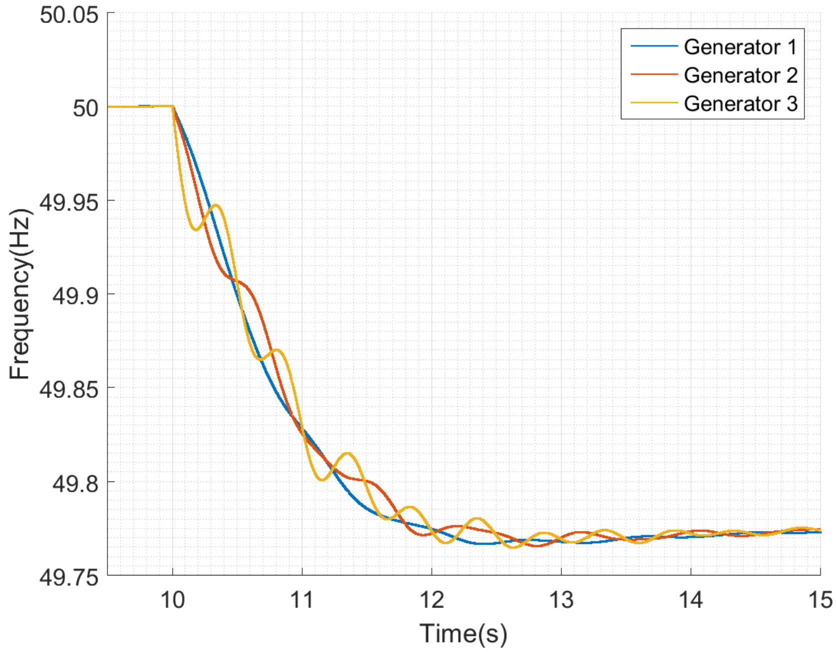

Figure 4.3: Generator Frequencies for 10% Load Connection

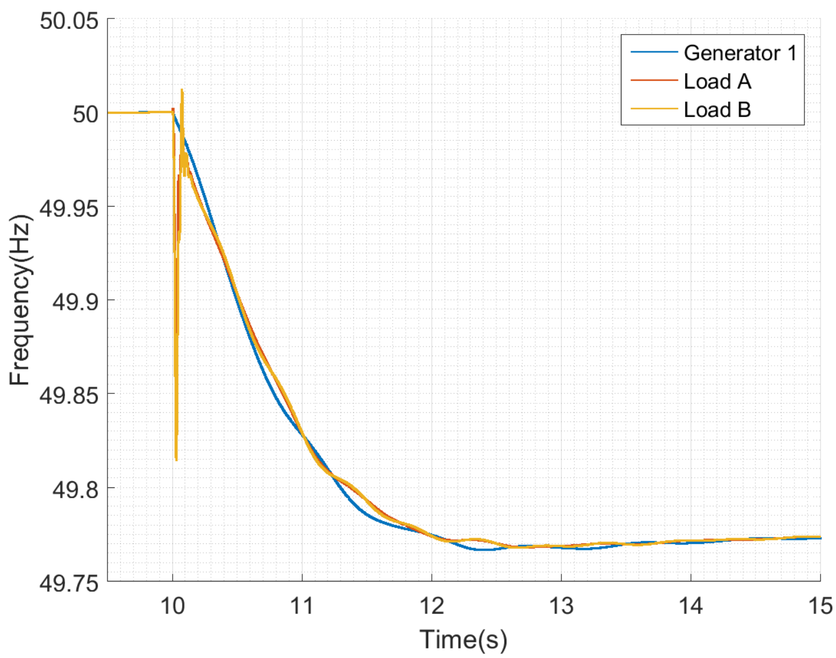

Figure 4.4: Frequencies in Generator 1, Load A and Load B

4.2 Modified Case

In this case, the P.M. Anderson test case is modified such that a wind farm consists of 20 wind turbine is connected to network. Wind farm is connected to Bus 5. Modified system is depicted in the Fig. 4.5. In this case, generator 2 and 3 are still assigned to same power values meanwhile generator 1 decreases its generation.

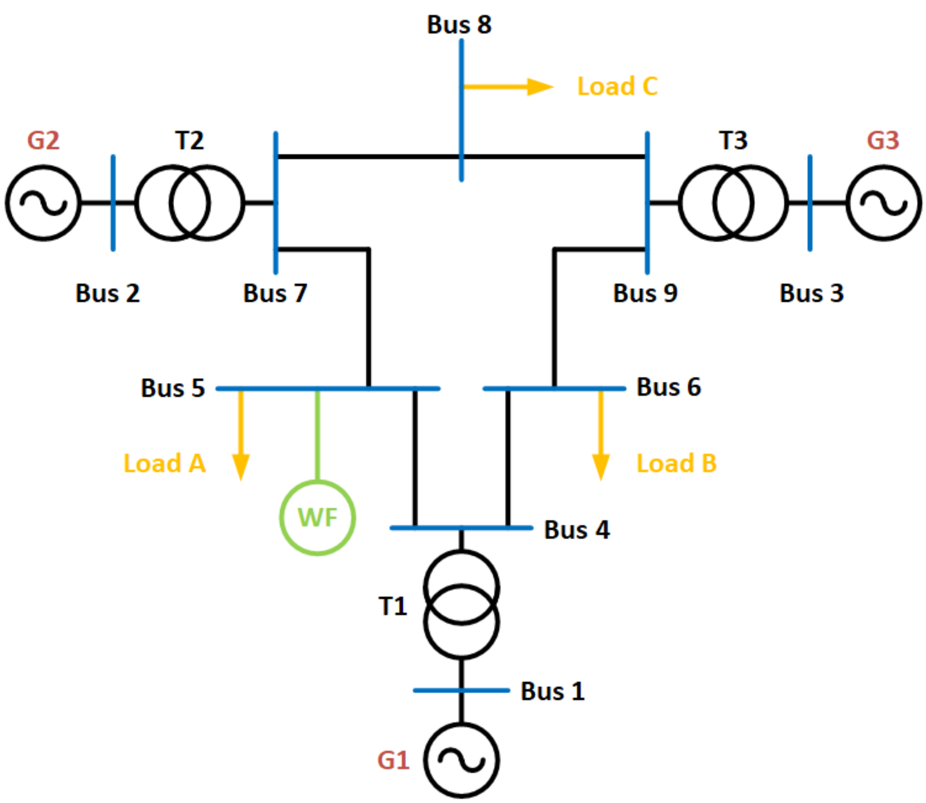

Figure 4.5: Modified System Single Line Diagram

4.2.1 Load Flow Analysis for Modified Case

Load flow analysis for modified case is listed in Table 4.5. The power injected from Bus 1 is decreased as expected. This can also be seen from the phase angle between 1 and 4. Phase angle difference between these buses decreased from $2.22°$ to $1.18°$.

Bus #	Bus Type	Voltage	Angle	Pg	Qg	Pl	Ql
1	SL	1.04	0	38.06	25.07	0	0
2	PV	1.025	11.33	163	6.65	0	0
3	PV	1.025	6.32	85	-10.86	0	0
4	PQ	1.0263	-1.18	0	0	0	0
5	PQ	0.9995	-1.54	0	0	125	50
6	PQ	1.0128	-2.43	0	0	90	30
7	PQ	1.0266	5.77	0	0	0	0
8	PQ	1.0164	2.62	0	0	100	35
9	PQ	1.0326	3.62	0	0	0	0

Table 4.5: Load Flow Results for Modified Case

4.2.2 Modified Case Frequency Response for Additional Load Connection

The modified base is very similar to the Base Case except for a wind farm located in Bus 5. The renewable energy system in this case can be considered as a negative load. Therefore, base case with decreased load is under discussion in this subsection. The same amount of load is taken into operation at Bus 6 and the frequency of the system is shown in Fig. 4.6.
Almost the same frequency response is observed in the system. The reason is that both systems have the same amount of stored kinetic energy. Another reason is the underutilization of the power system network. This can also be observed in the rate of change of frequencies in Fig. 4.7. Almost the same RoCoF values are observed in the system. This concludes that renewable energy penetration does not change frequency response of the system if the only change in the system is the inclusion of renewable energy system. Note that the renewable energy systems are intermittent energy sources. However, in this study,the source of the renewable energy system is assumed as constant. Therefore, the reason of frequency disturbance is load connection rather than the change in active power output of renewable systems.

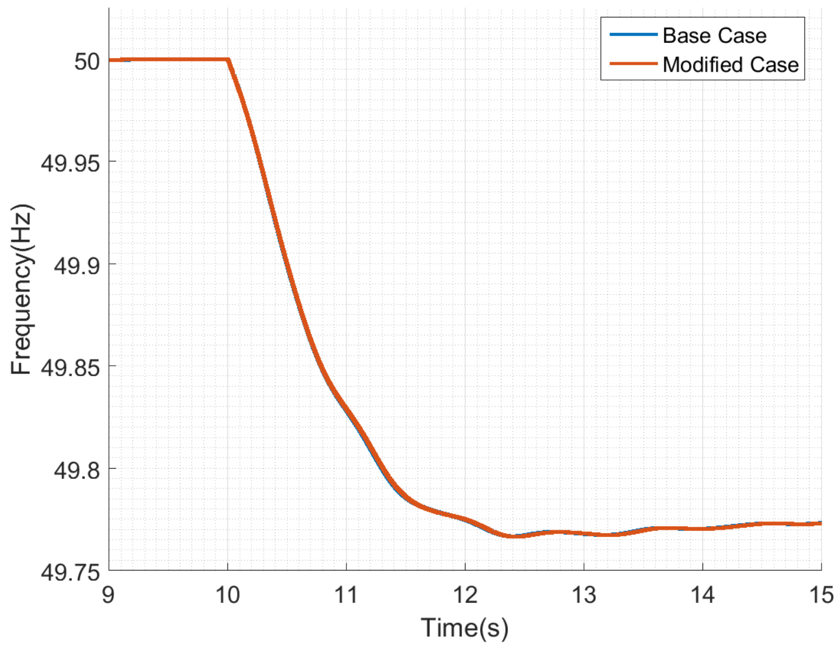

Figure 4.6: Comparison of Base Case and Modified Case Frequencies

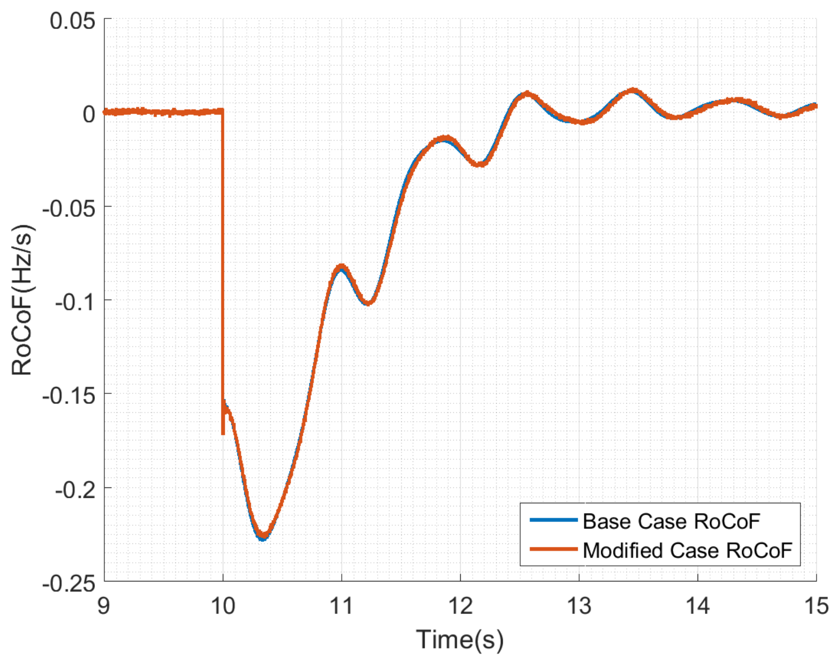

Figure 4.7: Comparison of Base Case and Modified Case Frequencies

4.3 Decommissioned Case

As seen in the Modified Case, the frequency response of the system does not change with renewable energy inclusion. However, it is inevitable that renewable energy systems will replace the conventional units in future. In this case, the smallest generator, generator 3, will be decommissioned. The decommissioned case diagram is shown in Fig. 4.8.

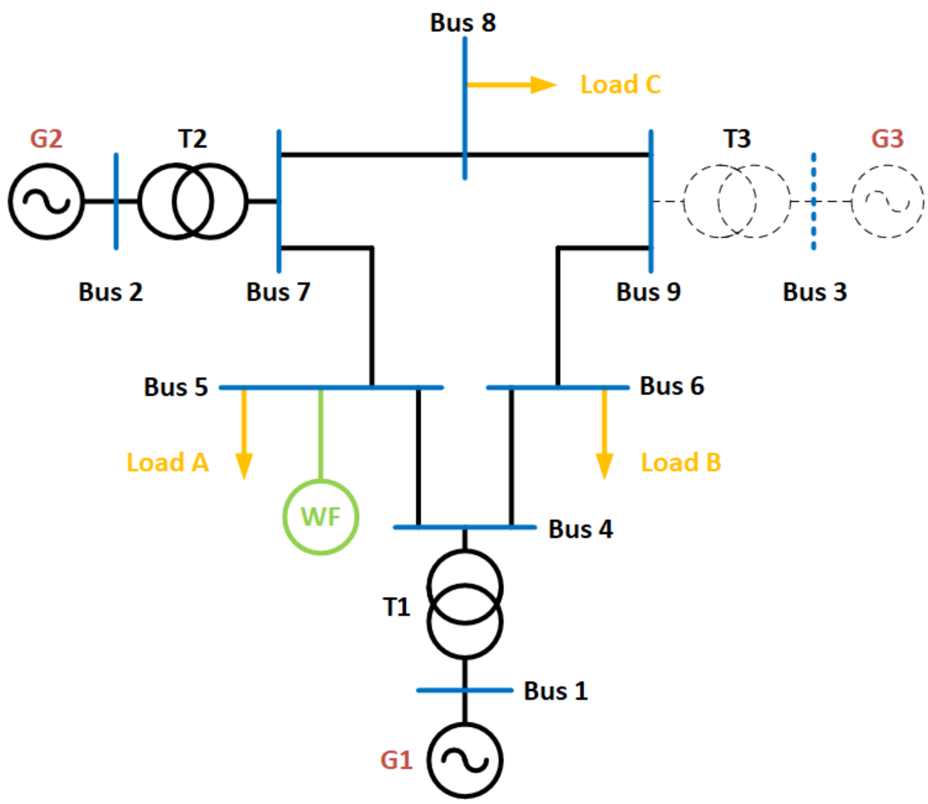

Figure 4.8: Comparison of Base Case and Modified Case Frequencies

Since the generator 3 is out of service, the stored kinetic energy is decreased in the system. Decommissioned system dynamical properties are updated and given in Table 4.6.

4.3.1 Load Flow Analysis for Decommissioned Case

Since the generator 3 is out of service, generator 1 loading will be increased. Load flow analysis for decommissioned case is given in Table 4.7.

Total System Load	315 MW
Generator Droop Settings	5%
Stored Kinetic Energy at Nominal Speed	3.004 GWs
Gen 1 Inertia Constant	9.5515 s
Gen 2 Inertia Constant	3.9216 s

Table 4.6: System Dynamical Properties

Bus #	Bus Type	Voltage	Angle	Pg	Qg	Pl	Ql
1	SL	1.04	0	121.76	16.26	0	0
2	PV	1.025	4.18	163	0.65	0	0
4	PQ	1.0332	-3.74	0	0	0	0
5	PQ	1.0083	-5.63	0	0	125	50
6	PQ	1.0224	-7.65	0	0	90	30
7	PQ	1.0294	-1.36	0	0	0	0
8	PQ	1.0207	-5.82	0	0	100	35

Table 4.7: Load Flow Results for Decommissioned Case

4.3.2 Decommissioned Case Frequency Response for Additional Load Connection

Same amount of additional load is taken into operation from Bus 6. System frequency response is observed and compared to Base Case and Modified Case in Fig. 4.9. As soon from the figure, the frequency nadir decreased from 49.77Hz to 49.65Hz. This is due to the decrease in the stored kinetic energy in the system. Due to the decommission of generator 3, the frequency decreases steeper following to load connection.This can also be observed RoCoF comparison given in Fig. 4.10.

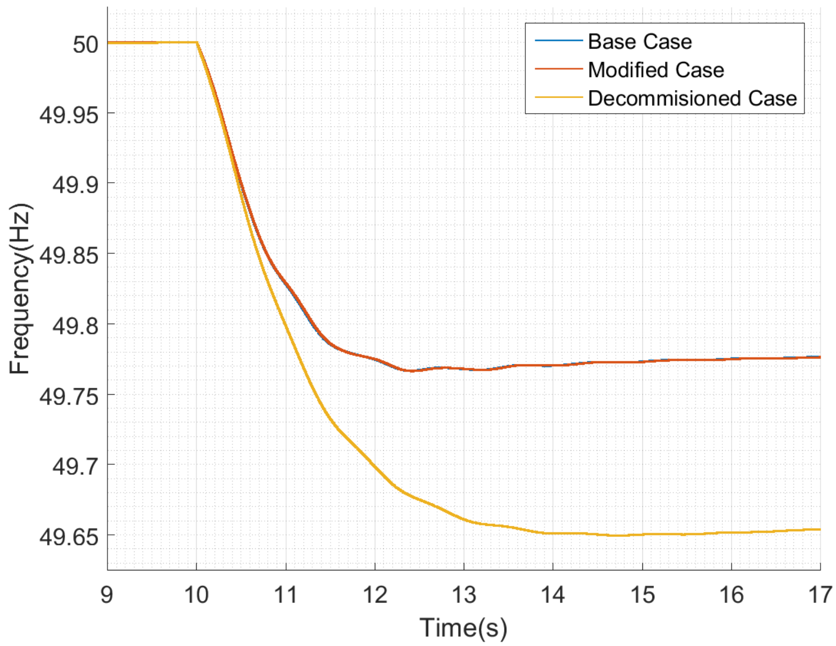

Figure 4.9: Comparison of Base Case,Modified Case and Decommissioned Case Frequency Responses

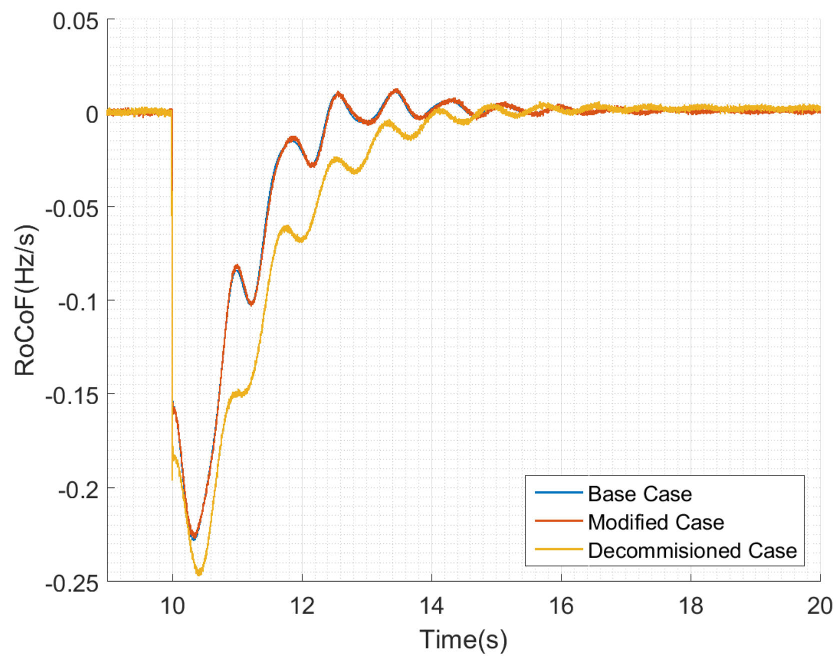

Figure 4.10: Comparison of Base Case,Modified Case and Decommissioned Case RoCoFs

REFERENCES

[1] International Renewable Energy Agency, *Renewable Energy Statistics 2017*. 2017.

[2] Eurostat, "Renewable energy in the EU-newsrelease," Tech. Rep. January, 2018.

[3] European Commission; and IRENA International Renewable Energy Agency, "Renewable Energy Prospects for the European Union," Tech. Rep. February, 2018.

[4] IRENA, "A Renewable Energy Roadmap," Tech. Rep. June, 2014.

[5] P. Kundur, *Power System Stability and Control*. McGraw-Hill,Inc.

[6] J. Eto, J. Undrill, P. Mackin, R. Daschmans, B. Williams, B. Haney, R. Hunt, J. Ellis, H. Illian, C. Martinez, M. OMalley, K. Coughlin, and K. Hamachi-LaCommare, "Use of Frequency Response Metrics to Assess the Planning and Operating Requirements for Reliable Integration of Variable Renewable Generation," no. December 2010, pp. LBNL–4142E, 2010.

[7] International Renewable Energy Agency (IRENA), *IRENA (2018), Renewable capacity statistics 2018*. 2018.

[8] European Commission, "Communication from the Commission to the European Parliament, the Council, the European economic and social Committee and the Committee of the Regions - 20 20 by 2020 - Europe's climate change opportunity," *COM (2008) 30 final*, p. Brussels, 2008.

[9] European Parliament, "Directive 2009/28/EC of the European Parliament and of the Council of 23 April 2009," *Official Journal of the European Union*, vol. 140, no. 16, pp. 16–62, 2009.

[10] REN21, *Renewables Global Futures Report*. 2017.

[11] A. Ipakchi and F. Albuyeh, "Grid of the future," *IEEE Power and Energy Magazine*, vol. 7, no. 2, pp. 52–62, 2009.

[12] D. Gautam, L. Goel, R. Ayyanar, V. Vittal, and T. Harbour, "Control strategy to mitigate the impact of reduced inertia due to doubly fed induction generators on large power systems," *IEEE Transactions on Power Systems*, vol. 26, no. 1, pp. 214–224, 2011.

[13] E. Muljadi, V. Gevorgian, and M. Singh, "Understanding Inertial and Frequency Response of Wind Power Plants Preprint," *2012 IEEE Power Electronics and Machines in Wind Applications (PEMWA)*, no. July, pp. 1–8, 2012.

[14] J. Van De Vyver, J. D. M. De Kooning, B. Meersman, L. Vandevelde, and T. L. Vandoorn, "Droop Control as an Alternative Inertial Response Strategy for the Synthetic Inertia on Wind Turbines," *IEEE Transactions on Power Systems*, vol. 31, no. 2, pp. 1129–1138, 2016.

[15] G. Lalor, J. Ritchie, S. Rourke, D. Flynn, and M. O'Malley, "Dynamic frequency control with increasing wind generation," *IEEE Power Engineering Society General Meeting, 2004.*, pp. 1–6, 2004.

[16] J. Ekanayake, "Control of DFIG wind turbines," *Power Engineer*, vol. 17, no. 1, pp. 28–32, 2003.

[17] J. Ekanayake and N. Jenkins, "Comparison of the response of doubly fed and fixed-speed induction generator wind turbines to changes in network frequency," *IEEE Transactions on Energy Conversion*, vol. 19, no. 4, pp. 800–802, 2004.

[18] J. Morren, S. de Haan, W. Kling, and J. Ferreira, "Wind Turbines Emulating Inertia and Supporting Primary Frequency Control," *IEEE Transactions on Power Systems*, vol. 21, no. 1, pp. 433–434, 2006.

[19] J. Morren, J. Pierik, and S. W. de Haan, "Inertial response of variable speed wind turbines," *Electric Power Systems Research*, vol. 76, no. 11, pp. 980–987, 2006.

[20] T. Ackermann, *Wind Power in Power Systems Wind Power in Power Systems Edited by*, vol. 8. 2005.

[21] S. Heier, *Grid Integration of Wind Energy*. 3 ed., 1998.

[22] H. Polinder, J. A. Ferreira, B. B. Jensen, A. B. Abrahamsen, K. Atallah, and R. a. McMahon, "Trends in Wind Turbine Generator Systems," *IEEE Journal of Emerging and Selected Topics in Power Electronics*, vol. 1, no. 3, pp. 174–185, 2013.

[23] Z. Chen, J. M. Guerrero, F. Blaabjerg, and S. Member, "A Review of the State of the Art of Power Electronics for Wind Turbines," *IEEE Transactions on Power Electronics*, vol. 24, no. 8, pp. 1859–1875, 2009.

[24] M. P. Kazmierkowski, R. Krishnan, and F. Blaabjerg, *Control in Power Electronics—Selected Problems*. New York: Academic, 2002.

[25] F. Blaabjerg, R. Teodorescu, M. Liserre, and A. V. Timbus, "Overview of control and grid synchronization for distributed power generation systems," *IEEE Transactions on Industrial Electronics*, vol. 53, no. 5, pp. 1398–1409, 2006.

[26] M. Chinchilla, S. Arnaltes, and J. C. Burgos, "Control of permanent-magnet generators applied to variable-speed wind-energy systems connected to the grid," *IEEE Transactions on Energy Conversion*, vol. 21, no. 1, pp. 130–135, 2006.

[27] T. Orłowska-Kowalska, F. Blaabjerg, and J. Rodríguez, *Advanced and intelligent control in power electronics and drives*. 2014.

[28] F. M. Gonzalez-longatt, "Activation Schemes of Synthetic Inertia Controller on Full Converter Wind Turbine (Type 4)," no. Type 4, 2015.

APPENDIX A

EK A

A.1 Örnek Kısım

Kısım içine yazılacaklar...